

# Experimental Investigation on the Retention of Soluble Particles by Pool Scrubbing

R. Vennemann

■,  
RWTH Aachen University,  
Templergraben 55,  
Aachen 52056, Germany  
e-mail: r.vennemann@fz-juelich.de

M. Klauck

■,  
RWTH Aachen University,  
Templergraben 55,  
Aachen 52056, Germany;  
Forschungszentrum Jülich GmbH,  
Jülich 52425, Germany  
e-mail: m.klauck@fz-juelich.de

H.-J. Allelein

■,  
RWTH Aachen University,  
Templergraben 55,  
Aachen 52056, Germany;  
Forschungszentrum Jülich GmbH,  
Jülich 52425, Germany  
e-mail: h.j.allelein@fz-juelich.de

*In the late stage of a severe loss-of-coolant accident, the pressure in the containment building of a nuclear power plant could rise beyond the design limits and thus endanger its structural integrity. Therefore, to avoid pressure failure, it may be necessary to perform controlled venting of the containment. During the event of an accident, a large amount of fission and activation products are released into the containment as airborne particles (aerosols). These particles are filtered during the venting process, usually with the help of wet filters, in order to keep risks to the surrounding environment to a minimum. Consequently, the knowledge of the retention processes in a water reservoir (pool scrubbing) is of central importance for such filtered containment venting systems and for reactor concepts in which water reservoirs are used for pressure reduction (e.g., condensation chamber of a boiling water reactor (BWR)). Investigations on pool scrubbing are carried out in the severe accident aerosol behavior (SAAB) test facility at the Juelich Research Center in the framework of a national project ("severe accident aerosol behavior-II"). SAAB is a unique large-scale facility with the ability to perform a great variation of experiments using various measurement tools. The influence of numerous parameters, such as the height of the water pool, solubility of aerosols and concentration of the retention capacity, is investigated by means of separate effect studies on both insoluble and soluble particles. This technical brief gives a detailed overview over the facility and includes example results of the first test series with soluble particles including cesium iodine (CsI). [DOI: 10.1115/1.4051250]*

**Keywords:** severe accident, source term, aerosols, experimental research, pool scrubbing

## 1 Introduction

In case of an at least temporarily uncontrolled loss-of-coolant accident in a water-cooled nuclear reactor, the reactor core can be partially exposed and destroyed. This leads to the release of radioactive fission products (aerosols and noble gases) first into the reactor cooling circuit and then into the containment atmosphere. In addition to the fission products and hydrogen, a large amount of steam also enters the containment, which leads to a pressure increase. In such an accident, there is a possibility that the pressure will reach the design limit of the containment and thus endanger its structural integrity. A failure of the containment should be avoided in any case because this would lead to an uncontrolled release of radioactive material into the environment. To prevent this, the containment should be depressurized before critical pressure limits are reached. Filtered containment venting systems are installed in numerous European nuclear power plants to reduce the pressure inside the containment with minimum release of radioactive fission products. One filter stage of this system usually consists of a wet filter, where airborne particles flow through a water seal. Therefore, a better understanding of the phenomenology of pool scrubbing is necessary in order to be able to make reliable assertions about the radioactive release into the environment. The condensation chamber of a boiling water reactor (BWR) not only serves to reduce pressure but also, in the sense of pool scrubbing, to retain fission products. In addition, water accumulations with small depths that have arisen during the course of an accident can also contribute to particle retention. [1,2]

Experimental studies in the past almost exclusively used insoluble particles [3]. Most of the pool scrubbing investigation focused on experiments with the insoluble substance  $\text{SnO}_2$  which is revealed in the passive and active systems on severe accident source term mitigation project [4]. Although it has been disclosed in the state-of-the-art review of fission product aerosol that the bulk of the aerosol released is likely to be soluble particles such as  $\text{CsI}$  and  $\text{CsOH}$  [5]. One of the most common integral test facilities in Europe "THAT" focused with their pool scrubbing investigations also on  $\text{SnO}_2$  [6]. Only the Poseidon Project at the Paul-Scherrer-Institute in Switzerland focused besides  $\text{SnO}_2$  also on iodine [7]. The first results of the investigation on the retention of soluble particles presented briefly in the following, generating data for model development or validation, is a part of future work to allow for robust simulations of pool scrubbing related phenomena.

## 2 Pool Scrubbing Phenomenon

Aerosol retention through pool scrubbing is expressed in terms of a decontamination factor (DF), which is defined as the ratio of aerosol mass flow rate at the inlet to that at the outlet.

$$\text{DF} = \frac{\dot{m}_{\text{in}}}{\dot{m}_{\text{out}}}$$

The path of the aerosols through the pool height may be split into three regions: injection, bubble rise, and pool surface and subsequently the overall DF is a multiplication of individual DFs and defined as in [1]

$$\text{DF} = \text{DF}_{\text{inj}} \times \text{DF}_{\text{rise}} \times \text{DF}_{\text{sur}}$$

**2.1 Injection Zone.** When the carrier gases along with the aerosol enter the pool at the orifice, the aerosols due to their inertia, impact on the liquid surface and are trapped, i.e., aerosol retention due to jet impaction. Gas injection velocity and the orifice diameter determine the flow regime. For this purpose, a non-dimensional Weber number is defined as [1]

$$\text{We} = \frac{\rho_l \times D_{\text{inj}} \times u_{\text{inj}}^2}{\sigma}$$

Manuscript received December 15, 2020; final manuscript received May 4, 2021; published online xx xx, xxxx. Assoc. Editor: Cecilia Martin-del-Campo.

If  $We < 105$ , the flow is in the globule regime, and if  $We > 105$ , the flow is in the jet regime. For the experiments presented in this technical brief ( $We = 9.104$ ), we restrict the discussion to only the globule regime. As the carrier gas enters the water pool through the orifice, an initial globule is formed. This globule, too large to be stable, breaks into smaller bubbles, and they rise like a swarm through the water pool. For the globular flow regime, aerosol size and density are the main contributors to the decontamination factor in the injection zone.

**2.2 Bubble Rise Zone.** In this region, the dynamics of aerosols trapped in the small rising bubbles is the primary contributor to the decontamination factor

$$DF_{\text{rise}} = \exp \left( \left( \frac{1}{V} \times \sum_n \int_A v_n(r) \times dA \right) \times \frac{H}{u_{\text{rise}}} \right)$$

The key factors are the residence time of the bubbles ( $H/u_{\text{rise}}$ ) and the relative motion of aerosols within the bubbles due to the following mechanisms: Diffusiophoresis, Thermophoresis, Sedimentation, Centrifugal impaction, and Brownian Diffusion. Each of the phenomena results in a relative velocity of aerosols with the bubble, causing the aerosols to drift toward the bubble interface (gas-liquid interface), where they are captured. Condensation/evaporation at the interface causes gradients in steam concentration and temperature, promoting aerosol transport due to diffusiophoresis and thermophoresis, respectively. Sedimentation accounts for the relative motion of aerosols due to gravitational acceleration, i.e., the heavier the particle, the better the retention. Centrifugal force on the aerosol is a result of the bubble's rotating motion. Bubble's rotating motions causes centrifugal forces on the aerosols inside, promoting migration toward the interface. Brownian diffusion results in aerosol transport from regions of high concentration to low concentration and is important for small particles ( $d < 0.1 \mu\text{m}$ ) [1,8].

Also, the particle size distribution within the rising bubbles impacts the gravitational settling, centrifugal impaction, and Brownian diffusion. Particle size distribution varies because of agglomeration and steam condensation on hygroscopic aerosols [1].

**2.3 Pool Surface Zone.** The bubbles rise to the surface of the water pool and rupture, producing microdroplets. The gas flow entrains some of these droplets, and others fall back due to gravity. Entrained droplets, in turn, transport fine aerosol particles [1].

To summarize, the factors affecting aerosol retention in a water pool are the inlet gas velocity, gas composition (steam concentration), gas temperature, particle Stokes number (aerosol density and size), hygroscopicity, or solubility of the aerosol material and pool height. In this work, the gas velocity, temperature, and composition (no steam) are kept constant. Only the impact of particle density and size distribution, solubility, and pool height on the pool scrubbing phenomenon is studied.

### 3 Facility Description

The severe accident aerosol behavior (SAAB) test facility (Fig. 1) consists of three parts— aerosol generation, aerosol conditioning, and tank with water reservoir. First, the aerosols are produced in the aerosol generating unit and then fed into the mixing chamber. In the mixing chamber, different aerosol streams are combined and further mixed with the carrier gas. The well-mixed aerosol is then led into the water reservoir, where aerosol particles are filtered. The properties of the aerosol are measured at the inlet and outlet of the water seal by sampling with measuring instruments, such as an electric low-pressure impactor (ELPI), an aerodynamic particle sizer or the scanning mobility particle sizer [3].

The tank in Fig. 1 is the heart of the test facility and contains the water seal. The tank itself is of modular design and consists of

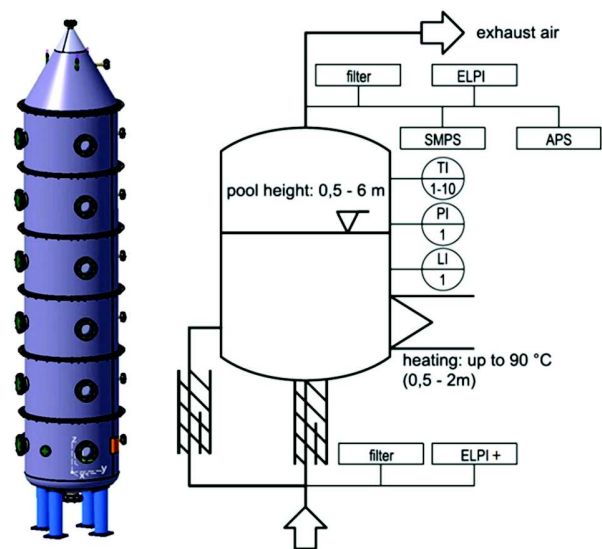


Fig. 1 SAAB test facility [3]

up to five separate segments, each segment measuring 1 m in height and 1.5 m in diameter. The aerosol flows into the lowest segment, through the tank, and out at the uppermost segment. It offers the possibility of varying the height of the water seal from a minimum of 0.5 m to a maximum of 5.5 m above the feed under identical sampling conditions. The maximum possible volume is  $10 \text{ m}^3$ . The top part of the test facility is conical and has provisions for the extraction of the filtered aerosol into an air filter system and a sampling line for measurements at the outlet. The right part of Fig. 1 shows the instrumentation of the vessel. The aerosol is directed into the SAAB container through an opening (1 in. diameter for the experiments presented here) located in the middle of the bottom segment. Additionally, it is possible to feed the aerosol downward or sideways to the container. Each segment, except the top one, has four flanged openings for instrumentation or optical access. The container and water reservoir can be heated to a temperature of  $90^\circ\text{C}$  by feeding steam. It is also equipped with a trace heating system for both the lower and the upper segments. As also shown in Fig. 1, a water-level sensor (see Fig. 1 longitude indicator (LI)), a pressure sensor ("PI"), and a humidity sensor ("MI") with integrated temperature sensor are installed in the upper, conical segment. In addition, a sample is taken at a height of about 0.65 m above the water surface.

### 4 Test Description and Execution

Cesium iodide (CsI) and cesium hydroxide (CsOH) are among aerosols present in the containment atmosphere during a late stage of a severe accident [1]. CsI (natural isotope) with a solubility of  $669.7 \text{ g/l}$  can only be used in the experiments after a number of precautions have been taken. CsOH is highly alkaline ( $\text{pH} = 14$  at  $500 \text{ g/l}$ ) and it is therefore extremely difficult to be utilized in experiments. Due to these limitations, substitutes were selected for the first series of experiments. Instead of CsI, sodium chloride (NaCl) with a water solubility of  $358 \text{ g/l}$  was chosen. Instead of CsOH, potassium acetate ( $\text{C}_2\text{H}_3\text{KO}_2$ ) with a water solubility of  $2560 \text{ g/l}$  was chosen [9]. After conducting the tests with NaCl, the facility was equipped with additional safety precautions to allow for the safe testing of CsI.

For the generation of soluble aerosols, a two fluid spraying system was used. The water-salt solution of the aerosol is mixed with  $\text{N}_2$  gas in the nozzle. The gas at the inlet to the nozzle system is under a higher pressure (5–10 bar). When it expands through the nozzle to a lower pressure ( $\sim 1 \text{ bar}$ ), the gas accelerates. The impulse transfer between gas and liquid breaks the liquid into fine

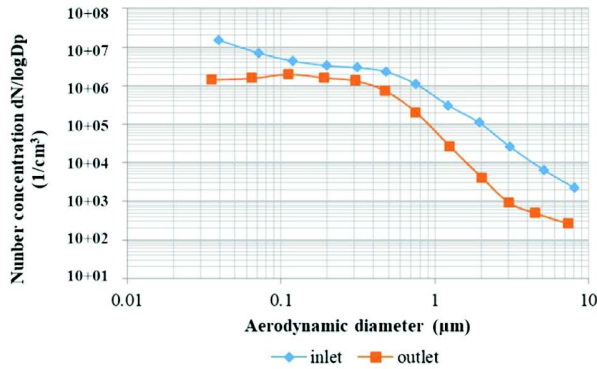


**Fig. 2 Particle size class number concentration of NaCl aerosol measured at the inlet and outlet for a flow rate of 250 g/h and a pool height of 1.5 m**

droplets. During the subsequent evaporation of the liquid droplets by means of a heating system, the particles crystallize and are then mixed with the carrier gas stream (N<sub>2</sub>) to produce the desired aerosol.

In addition to the spraying system for soluble particles, the SAAB facility also uses a particle disperser with brush, which produces insoluble particles, such as SnO<sub>2</sub>. A detailed description can be found in the SAAB final project report [3].

The parameters of the experimental test matrix are:

- solubility (NaCl, C<sub>2</sub>H<sub>3</sub>KO<sub>2</sub>, CsI)
- aerosol concentration (NaCl, C<sub>2</sub>H<sub>3</sub>KO<sub>2</sub>, CsI)
- pool height (NaCl, C<sub>2</sub>H<sub>3</sub>KO<sub>2</sub>, CsI)
- injection speed (CsI, NaCl)

The height of the water above the aerosol inlet is referred to here as the water level or pool height. The water heights considered in the experiments are 1.5 m and 5.5 m for NaCl and 1.5 m to 5.5 m for CsI. The aerosol concentration in the carrier gas is varied by changing the mass flow of the liquid solution into the two fluid spraying system (150–300 g/h). The N<sub>2</sub> carrier gas volume flow is kept constant in all experiments (20 m<sup>3</sup>/h). The gas temperature before the inlet is 30 °C, the water temperature averages 22 °C, and the sampling temperature is 60 °C to keep the relative humidity at a similar level as at the inlet. All tests are repeated at least two times to ensure the reproducibility of results.

**Table 1 Uncertainties of the measured retention efficiencies**

di (μm)	0.1	0.2	0.3	0.5	0.8	1.2	2.0	3.1	5.1
− $\bar{\eta}$	0.2%	0.3%	0.5%	0.4%	0.4%	0.3%	0.2%	0.4%	2.1%
+ $\bar{\eta}$	0.2%	0.3%	0.5%	0.4%	0.3%	0.3%	0.2%	0.3%	0.9%

## 5 Results

About 100 experiments were performed at the SAAB facility to study the aerosol retention capability of pool scrubbing for multiple combinations of test parameters— aerosol material (solubility), aerosol concentration (injection rate), and pool height. Presenting the results of all the experiments is outside the scope of this technical brief; therefore, we restrict the discussion on retention efficiency of aerosols only for the following cases:

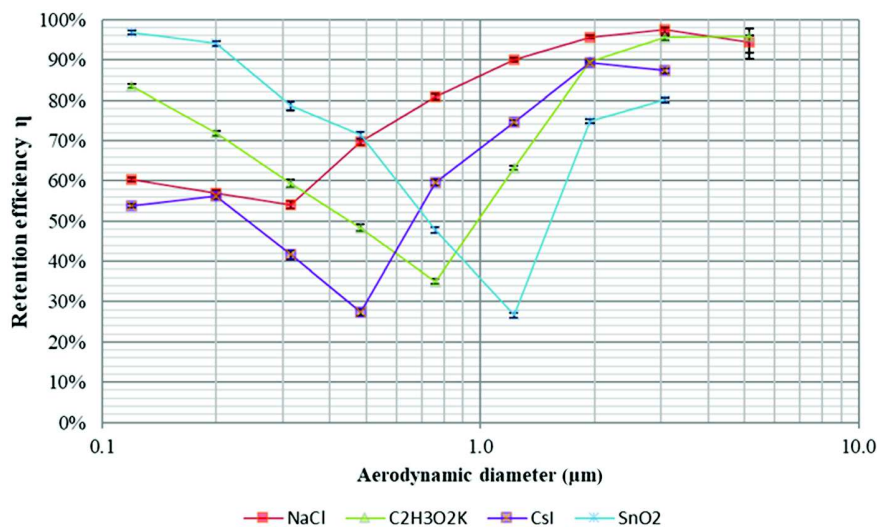
- NaCl aerosol for four concentrations (mass flow rate of the liquid solution: 150 g/h, 200 g/h, 250 g/h, and 300 g/h), at two pool heights (1.5 m and 5.5 m).
- CsI at 250 g/h for five pool heights—1.5 m, 2.5 m, 3.5 m, 4.5 m, and 5.5 m.
- Soluble aerosols (NaCl, C<sub>2</sub>H<sub>3</sub>KO<sub>2</sub>, and CsI) and Insoluble aerosol (SnO<sub>2</sub>) at 250 g/h and for a pool height of 1.5 m.

Figure 2 shows an example measurement output of the ELPs. It shows the number concentrations for a basin height of 1.5 m before (blue) entry into and after (orange) exit from the water reservoir. Each measuring point is assigned to a certain size class. The number of concentration describes the quantity of particles of a certain size class per cm<sup>3</sup> counted during the experiment. With the help of this data, conclusions can ultimately be drawn about the retention efficiency described in more detail below.

If  $DF = 1$ , no retention has taken place. In the case of especially large  $DF$  values where retention is mainly the result of large particles, the figures are not very clear. More illustrative is the so-called retention efficiency ( $\eta$ ), which is linked to  $DF$  as

$$\eta = 1 - \frac{1}{DF}$$

Therefore,  $\eta$  is preferred in this document for the representation of the retention. The equation of the retention efficiency can thus also be set as a function of the mass flow or the measured mass concentration  $cm$ . This leads to the following equation:



**Fig. 3 Particle size class retention efficiency for soluble (NaCl, CH<sub>3</sub>CO<sub>2</sub>K, CsI) and insoluble aerosols (SnO<sub>2</sub>) for an injection rate of 250 g/h and pool height of 1.5 m**



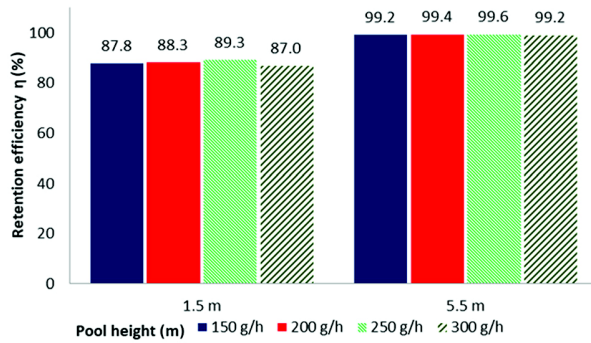


**Fig. 4 Impact of aerosol concentration (injection rate) on retention efficiency for NaCl aerosol at pool heights of 1.5 m and 5.5 m**

$$\eta = 1 - \frac{C_{m \text{ out}}}{C_{m \text{ in}}}$$

The used measurement device ELPI measures and calculates the mass concentration for each diameter as follows [10]:

$$C_{m, \text{elpi}, i} = \frac{d_i^3 \times \pi \times \gamma \times \rho}{X_i \times 6}$$

After 100 and more experiments have been carried out on the SAAB system, it is finally possible to calculate and predict the measurement uncertainty of the SAAB facility. For this purpose, the model of the Gaussian error propagation law [11] was used and applied in the following equation:

$$s_{n, i}^2 = \frac{\partial C_{\text{elpi}, i}}{\partial d_{\text{stk}, i}} \times s_{d_{\text{stk}, i}}^2 + \frac{\partial C_{\text{elpi}, i}}{\partial \gamma} \times s_{\gamma}^2$$

These preparations finally lead to the following equation to determine the uncertainty as:

$$\eta = 1 - \frac{C_{m \text{ out}, i} \pm s_{n \text{ out}, i}}{C_{m \text{ in}, i} \pm s_{n \text{ in}, i}}$$

If the largest and smallest quotients of the equation are used, the raw values of the uncertainty are obtained. Because particles

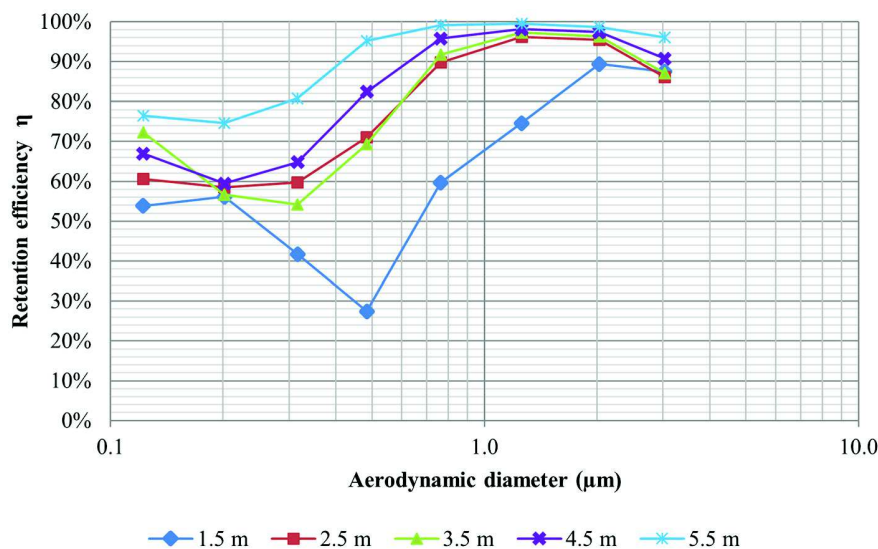
with a larger diameter have more mass, their uncertainty is greater. However, only measured values up to max.  $5 \mu\text{m}$  are included in the following diagrams. The calculated uncertainties of the measured values are shown as an example in Fig. 3. Table 1 displays the uncertainties in positive and negative directions for diameters, which could be measured with the ELPI.

Figure 4 shows the integral retention efficiencies over the feed concentration for sodium chloride. The concentration variations are shown both for a water column height of 1.5 m and for a height of 5.5 m. The different concentrations differ in color. Based on these results, a concentration variation due to a change in the feed mass flows of 150 g/h up to a concentration of 300 g/h leads to almost identical results. For a height of 5.5 m, the retention efficiency for all concentrations is approx.  $99.4\% \pm 0.2\%$ . For a height of 1.5 m, the results of the retention efficiency are around  $88\% \pm 1\%$ .

Figure 5 shows the preliminary results of the first experiments with CsI. The retention efficiency for each size class is shown for a water-level height of 1.5 m–5.5 m. The influence of height on the retention efficiency is clearly recognizable, especially a substantial increase in filtration efficiency between pool heights of 1.5 m and 2.5 m for all particle sizes; for the smaller particles ( $0.1\text{--}1.0 \mu\text{m}$ ), a significant rise in retention efficiency between pool heights of 4.5 m and 5.5 m (Fig. 5).

A comparison of different substances tested in the SAAB facility is shown in Fig. 3. The retention efficiency  $\eta$  for a pool height of 1.5 m is graphed over the particle diameter. The height of 1.5 m was chosen because the greatest difference in retention can be recognized at this level. Similar size distribution of aerosol feed is maintained to ensure the comparability of retention efficiency for different soluble materials. The blue curve shows the course of the size classes of the retention efficiency for NaCl, the red curve for  $\text{C}_2\text{H}_3\text{KO}_2$ , the green curve for CsI, and the purple curve for the insoluble SnO2 for comparison. All four substances show a substance-specific minimum in the filter efficiency (so-called filter gap). For sodium chloride, the minimum is 54% at a particle diameter of about  $0.3 \mu\text{m}$ , for potassium acetate 35% at about  $0.8 \mu\text{m}$ , for cesium iodine 27% at  $0.5 \mu\text{m}$ , and finally for tin dioxide 26% at a particle diameter of about  $1.2 \mu\text{m}$ . Contrary to our expectations, the substance with the highest solubility was not retained the best.

Another unexpected result is that the insoluble SnO2 exhibits the best retention for particles sizes lower than  $0.5 \mu\text{m}$ . With decreasing the density, the retention efficiency increases for all substances, except for potassium acetate. When considering



**Fig. 5 Particle size class retention efficiency for CsI aerosol at 250 g/h for different pool heights—1.5 m, 2.5 m, 3.5 m, 4.5 m, and 5.5 m**

diameters above  $0.7\text{ }\mu\text{m}$ , NaCl ( $2.16\text{ g/cm}^3$  [9]) is retained the best, followed by CsI ( $4.51\text{ g/cm}^3$  [9]). The material with the highest density,  $\text{SnO}_2$  ( $6.95\text{ g/cm}^3$  [9]), shows the worst performance of the three from this size class up.

## 6 Summary and Conclusion

The investigations were carried out at the SAAB test facility in Research Center Juelich, to understand the impact of aerosol material solubility on pool scrubbing retention efficiency. For this purpose, three soluble materials—NaCl,  $\text{C}_2\text{H}_3\text{KO}_2$ , and CsI—and one insoluble substance— $\text{SnO}_2$ —were used. In addition to the material solubility, the parameters investigated were the pool height ( $1.5\text{ m}$ – $5.5\text{ m}$ ) and aerosol mass concentration at the inlet orifice ( $150\text{ g/h}$ – $300\text{ g/h}$ ). Integral as well as particle size-wise ( $dp \sim 0.04\text{ }\mu\text{m}$ – $8\text{ }\mu\text{m}$ ) retention efficiencies are presented. The estimation of measurement uncertainties is still a work in progress.

For NaCl aerosol, the retention efficiency remained independent of the inlet mass concentration, contrary to the expected behavior of enhanced retention due to a higher number of particle–bubble surface interactions.

For the same mass concentration and pool height, NaCl, having a comparatively lower density than CsI (a higher number of particles), was retained better in the water pool. Between NaCl and CsI, Brownian diffusion due to particle number concentration overwhelms gravitational settling and Centrifugal impaction proportional to particle density.

For insoluble and soluble aerosols, the highest retention occurs within the first  $1.5\text{ m}$  of pool height, confirming that the jet impaction at the orifice is the dominant phenomenon. Despite our expectations, solubility was not a key factor in pool scrubbing. Rather, density and, therefore, number concentration seem to be of more importance. For NaCl and CsI aerosols, with increasing pool heights, the residence time of the aerosol in water increases, and consequently, the retention efficiency increases.

The results from this work indicate that an integral DF (based on mass) does not reveal an accurate picture of aerosol retention; the larger, heavier particles are best filtered, thereby masking the poor retention of small, respirable aerosols.

Future work will focus on studying the retention efficiency of pool scrubbing methods for mixed component aerosols and different gas compositions and temperatures. Furthermore, investigations on bubble behavior in SAAB are planned to gain deeper insights into the pool scrubbing phenomenon.

## Funding Data

- Federal Ministry of Economics and Energy (Grant no. 1501551; Funder ID: ■).

## Nomenclature

$c$	= concentration, $\text{kg/m}^3$
$D/d$	= diameter, $\text{m}$
$H$	= height, $\text{m}$
$\dot{m}$	= mass flow, $\text{kg/s}$
$r$	= radius, $\text{m}$
$s$	= standard deviation/uncertainty
$u$	= velocity, $\text{m/s}$
$v$	= depletion mechanism velocity, $\text{m/s}$
$V$	= volume, $\text{m}^3$
$X$	= measurement accuracy

## Greek Symbols

$\gamma$	= dilution factor
$\eta$	= retention efficiency; $\left(1 - \frac{1}{\text{DF}} = 1 - \frac{c_{m\text{ out}}}{c_{m\text{ in}}}\right)$
$\rho$	= density, $\text{kg/m}^3$
$\sigma$	= surface tension, $\text{N/m}$

## Nondimensional Numbers

DF = decontamination factor;

$$\left(\frac{\dot{m}_{\text{in}}}{\dot{m}_{\text{out}}} = \text{DF}_{\text{inj}} \times \text{DF}_{\text{rise}} \times \text{DF}_{\text{sur}}\right)$$

$$\text{We} = \text{Weber number}; \left(\frac{\rho_l \times D_{\text{inj}} \times v_{\text{inj}}^2}{\sigma}\right)$$

## Subscripts or Superscripts

elpi	= electric low-pressure impactor
in	= in/inlet
inj	= injection
l	= liquid
m	= mass(-based)
out	= out/outlet
rise	= (bubble) rising zone
stk	= Stokes
sur	= surface

## Acronyms

BWR	= boiling water reactor
$\text{C}_2\text{H}_3\text{KO}_2$	= potassium acetate
CsI	= cesium iodine
CsOH	= cesium hydroxide
ELPI	= electric low-pressure impactor
MI	= hygrometer
$\text{N}_2$	= nitrogen
NaCl	= sodium chloride
PI	= pressure indicator
SAAB	= severe accident aerosol behavior (facility)
$\text{SnO}_2$	= tin dioxide

## References

- Allelein, H.-J., Auvinen, A., Ball, J., Güntay, S., Herranz, L., Hidaka, A., Jones, A. V., Kissane, M., Powers, D., and Weber, G., 2009, "State of the Art Report on Nuclear Aerosols," *Org. Econ. Co-Oper. Dev.*, **388**(■), pp. 21–47.
- Jacquemain, D., Güntay, S., Basu, S., Sonnenkalb, M., Lebel, L., Allelein, H.-J., Liebana Martinez, B., Eckardt, B., and Ammirabile, L., 2014, "OECD/NEA/CSNI Status Report on Filtered Containment Venting," *Org. Econ. Co-Oper. Dev.*, **147**(■), pp. 65–75.
- Allelein, H.-J., Kobalz, J., Kubelt, C., Küpper, J., Steffen, P.-M., and de Winter, R., 2018, *Aerosolverhalten bei schweren Störfällen—Severe Accident Aerosol Behaviour—Reactor Safety Research Project No.: 1501454*, Vol. 253, RWTH Aachen University, Aachen, Germany, pp. 7–71.
- Dehbi, A., Suckow, D., and Güntay, S., 2000, *Aerosol Retention in Low-Subcooling Pools Under Realistic Accident Conditions*, Paul-Scherrer-Institute, Villigen, Switzerland, p. 13.
- Swiderska-Kowalczyk, M., Escudero-Berzal, M., Marcos-Crespo, M., Martin-Espigares, M., and Lopez-Jimenez, J., 1995, "State-of-the-Art Review on Fission Products Aerosol Pool Scrubbing Under Severe Accident Conditions: Final Report," ■, **228**(■), pp. 1–83.
- Freitag, M., Schmidt, E., Colombet, M., and von Laufenberg, B., 2018, *Aerosolrückhaltung in einer Wasservorlage - Pool Scrubbing. Versuchsserie WH-25 - WH-27*, Becker Technologies GmbH, Eschborn, Germany, p. 229.
- Albiol, T., Herranz, L., Riera, E., Dalibart, C., Lind, T., Del Corno, A., Kärkelä, T., Losch, N., Azambre, B., Mun, C., and Cantrel, L., 2018, "Main Results of the European PASSAM Project on Severe Accident Source Term Mitigation," *Ann. Nucl. Energy*, **116**, pp. 42–56.
- Dehbi, A., and Güntay, S., 1994, *Simulation of Pool Scrubbing Experiments Using BUSCA*, Paul Scherrer Institute, ■, p. 16.
- Koppisch, D., and Gabriel, S., 2011, *GESTIS-Stoffdatenbank*, Institut für Arbeitsschutz der Deutschen Gesetzlichen Unfallversicherung, ■, ■, accessed ■, <https://gestis.dguv.de/>.
- , 2010, *ELPI+TM User's Manual—Version 1.23*, Dekati, ■, p. 80.
- Barlow, R., 1989, *A Guide to the Use of Statistical Methods in the Physical Sciences*, Wiley, ■, p. 204.